

AD-A084 814

ROYAL AIRCRAFT ESTABLISHMENT FARNBOROUGH (ENGLAND) F/8 1/3  
OPENING-MODE STRESS INTENSITY FACTORS FOR TWO UNEQUAL CRACKS AT--ETC(U)  
AUG 79 D P ROOKE, J TWEED  
RAE-TR-79105

DRIC-BR-71448

NL

UNCLASSIFIED

1 OF 1  
AD-A  
084814




END  
DATE  
FILMED  
6-80  
DTIC

TR 79105

ADA084814

UNLIMITED

TR 79105

BR71448

2



ROYAL AIRCRAFT ESTABLISHMENT

\*

Technical Report 79105

August 1979

LEVEL

OPENING-MODE STRESS INTENSITY  
FACTORS FOR TWO UNEQUAL  
CRACKS AT A HOLE

by

D.P. Rooke

J. Tweed

DTIC  
ELECTE  
FEB 28 1980  
S D C

\*

Procurement Executive, Ministry of Defence  
Farnborough, Hants

DDG FILE COPY

UNLIMITED

UDC 539.4.014.11 : 539.211 : 539.219.2 : 539.4.013.3

34 APR 1979  
12/31

ROYAL AIRCRAFT ESTABLISHMENT

4 Technical Report, 9105

Received for printing 15 August 1979

11/11

OPENING-MODE STRESS INTENSITY FACTORS FOR TWO UNEQUAL CRACKS AT A HOLE.

by

D. P. Rooke

J. Tweed\*

18 D  
11/11

SUMMARY

An integral-transform method is used to solve the elastic problem of two collinear cracks at the edge of a hole in a sheet. Both uniform loadings on the sheet remote from the crack and loadings on the perimeter of the hole are considered. Since in all cases the loadings are symmetrical about the crack-line, only the opening-mode stress intensity factors are non-zero; these factors are calculated. An approximate procedure is examined for obtaining stress intensity factors for two cracks at a hole from that for one crack.

Departmental Reference: Mat 386

Copyright

©

Controller HMSO London

1979

\* Old Dominion University, Norfolk, Va, USA

This document has been approved for public release and sale; its distribution is unlimited.

210450

LIST OF CONTENTS

	<u>Page</u>
1 INTRODUCTION	3
2 BASIC THEORY	4
3 NUMERICAL PROCEDURE	5
4 LOADING FUNCTIONS	6
4.1 Uniaxial tensile stress	7
4.2 Biaxial tensile stress	7
4.3 Point forces	7
4.4 Constant pressure	7
5 RESULTS	8
5.1 Uniaxial tensile stress	8
5.2 Biaxial tensile stress	8
5.3 Point forces	9
5.4 Constant pressure	9
6 DISCUSSION	9
7 CONCLUSIONS	12
Tables 1 to 8	13
List of symbols	21
References	22
Illustrations	Figures 1-6
Report documentation page	inside back cover

Accession For	
NTIS GRA&I	<input checked="" type="checkbox"/>
DDC TAB	<input type="checkbox"/>
Unannounced	<input type="checkbox"/>
Justification	<input type="checkbox"/>
By _____	
Distribution/ _____	
Availability _____	
Dist	Available for special
A	

## 1 INTRODUCTION

Cracks in the engineering materials used in aircraft structures may be present at manufacture or they may appear during the service life. Indeed, recent design requirements for 'damage-tolerant' airframe structures are often based on the assumption that cracks are present at the start of service life. In order to ensure safety and to optimize inspection schedules, it is necessary to know both the residual strength of the cracked structure and the rate at which the crack will grow under the action of service loads. Both of these depend upon the stress intensity factor which governs the stress-field at the tip of the crack.

Examination of failures (see for instance Kirkby<sup>1</sup>) shows that both service and test failures frequently occur as a result of cracks which originate in regions of high stress concentration such as the edges of holes or cut-outs. The first stress intensity factor solution available for radial cracks from a circular hole was that due to Bowie<sup>2</sup>. His solution which is restricted to one crack or two cracks of equal length is not very accurate for short cracks owing to the limitations of the method used. Knowledge of the growth of short cracks is, however, of technological importance, since much of the fatigue life of a structure is spent while the cracks are short. Recently an accurate method of solution for one crack at the edge of a hole has been obtained by Tweed and Rooke<sup>3</sup>; the method can be applied to any configuration with a stress distribution which is symmetric about the crack line. This method has now been extended by Tweed and Rooke<sup>4</sup> to problems with two cracks of different lengths, a common practical configuration.

In this Report the opening-mode stress intensity factors are calculated for two collinear radial cracks of different lengths at the edge of a circular hole in a large sheet which is subjected to different load distributions. Four distributions are considered; they are (see Fig 1)

- (i) a uniform uniaxial tensile stress remote from the cracks acting in a direction perpendicular to the crack line,
- (ii) a uniform biaxial tensile stress remote from the cracks with components acting parallel and perpendicular to the crack-line,
- (iii) two opposing forces acting perpendicular to the crack line at points on the edge of the hole, and
- (iv) a uniform pressure acting around the perimeter of the hole (but not on the crack faces); the stress intensity factor for a uniform

pressure acting around the perimeter of the hole and on the crack faces is the same as that for case (ii) if the two components of the biaxial stress are equal to the pressure.

In section 6 it is shown that for all cases the predominant parameter in determining the stress intensity factor is the total crack-length, *i.e.* the tip-to-tip distance. This leads to a relatively simple graphical relationship between results for two cracks and results for one crack. An approximation which has been suggested (see for example Broek<sup>5</sup>) for obtaining stress intensity factors for two equal-length cracks from that for one crack is examined in the light of this relationship and its accuracy assessed.

## 2 BASIC THEORY

The hole is defined in plane polar co-ordinates  $(\rho, \theta)$  by  $0 \leq \rho \leq R$ ,  $0 \leq \theta \leq 2\pi$  and the cracks by  $R \leq \rho \leq cR$ ,  $\theta = 0$  and  $R \leq \rho \leq bR$ ,  $\theta = \pi$  (see Fig 2). The crack lengths are denoted by  $l_1$  and  $l_2$  respectively where  $l_1 = (b - 1)R$  and  $l_2 = (c - 1)R$ . In general, the normal stresses along the crack site, in the uncracked body due to the applied loads, are given<sup>4</sup> by

$$\text{and } \left. \begin{aligned} \sigma_{\theta\theta}(\rho, 0) &= -p_0 f(r), & 1 \leq r \leq c \\ \sigma_{\theta\theta}(\rho, \pi) &= -p_0 g(r), & 1 \leq r \leq b, \end{aligned} \right\} \quad (1)$$

where  $r = \rho/R$  and  $p_0$  has the dimensions of stress. The opening-mode stress intensity factors for the two tips at  $(bR, \pi)$  and  $(cR, 0)$  are given<sup>4</sup>, for the crack of length  $l_1$ , by

$$\left. \begin{aligned} \frac{K_I}{p_0 \sqrt{\pi l_1}} &= \frac{\sqrt{2}}{b-1} h(-b), \\ \text{and, for the crack of length } l_2, \text{ by} \\ \frac{K_I}{p_0 \sqrt{\pi l_2}} &= -\frac{\sqrt{2}}{c-1} h(c). \end{aligned} \right\} \quad (2)$$

The function  $h(t)$  must satisfy the coupled singular integral equations<sup>4</sup>

$$\frac{1}{\pi} \int_{-b}^{-1} \frac{h(t)M(r,t)dt}{\sqrt{(-1-t)(t+b)}} + \frac{1}{\pi} \int_1^c \frac{h(t)M(r,t)dt}{\sqrt{(c-t)(t-1)}} = \begin{cases} -g(-r), & -b < r < -1 \\ -f(r), & 1 < r < c, \end{cases} \quad (3)$$

with conditions

$$h(1) = h(-1) = 0. \quad (4)$$

The kernel  $M(r,t)$  is singular and given<sup>4</sup> by

$$M(r,t) = \frac{1}{t-r} + k(r,t). \quad (5)$$

The non-singular part  $k(r,t)$  is given<sup>4</sup> by

$$k(r,t) = \frac{(1-t^2)^2}{t(1-rt)^3} - \frac{t(1-t^2)}{(1-rt)^2} - \frac{t}{1-rt} + \frac{1-t^2}{r^2t}. \quad (6)$$

### 3 NUMERICAL PROCEDURE

The equations (3) and (4) are reduced to a system of simultaneous linear algebraic equations by using a procedure developed by Erdogan and Gupta<sup>6</sup>. Let

$$u_j = \begin{cases} \cos [(2j-1)\pi/(2m)] & j = 1, 2, \dots, m \\ u_{j-m} & j = m+1, \dots, 2m; \end{cases} \quad (7)$$

$$v_j = \begin{cases} \cos (j\pi/m) & j = 1, 2, \dots, m \\ v_{j-m} & j = m+1, \dots, 2m \end{cases}, \quad (8)$$

$$t_j = \begin{cases} (b-1)u_j/2 - (b+1)/2, & j = 1, 2, \dots, m \\ (c-1)u_j/2 + (c+1)/2, & j = m+1, \dots, 2m \end{cases} \quad (9)$$

$$r_j = \begin{cases} (b-1)v_j/2 - (b+1)/2, & j = 1, 2, \dots, m \\ (c-1)v_j/2 + (c+1)/2, & j = m+1, \dots, 2m. \end{cases} \quad (10)$$

Equations (3) and (4) can now be reduced to the following linear algebraic system:

$$\left. \begin{aligned}
 \frac{1}{m} \sum_{j=1}^{2m} h(t_j) M(r_k, t_j) &= -g(-r_k), & k = 1, 2, \dots, m-1 \\
 \frac{1}{m} \sum_{j=1}^m h(t_j) (-1)^j \sqrt{\frac{1+u_j}{1-u_j}} &= 0 \\
 \frac{1}{m} \sum_{j=1}^{2m} h(t_j) M(r_k, t_j) &= -f(r_k), & k = m+1, \dots, 2m-1 \\
 \frac{1}{m} \sum_{j=1}^m h(t_j) (-1)^j \sqrt{\frac{1-u_j}{1+u_j}} &= 0.
 \end{aligned} \right\} (11)$$

The solution  $h(t_j)$  of these equations is used in a Gauss-Chebyshev interpolation formula to determine the stress intensity factors as follows:

$$\frac{K_I}{p_0 \sqrt{\pi \ell_1}} = \frac{\sqrt{2}}{m(b-1)} \sum_{j=1}^m (-1)^j h(t_j) \sqrt{\frac{1-u_j}{1+u_j}};$$

for the crack of length  $\ell_1$ , and (12)

$$\frac{K_I}{p_0 \sqrt{\pi \ell_2}} = \frac{\sqrt{2}}{m(c-1)} \sum_{j=m+1}^{2m} (-1)^j h(t_j) \sqrt{\frac{1+u_j}{1-u_j}}$$

for the crack of length  $\ell_2$ .

#### 4 LOADING FUNCTIONS

In order to solve equations (11) the loading functions  $g(-x_k)$  and  $f(x_k)$  must be known. These are derived from the stress fields along the crack-site in the uncracked configuration.

#### 4.1 Uniaxial tensile stress

For a uniform uniaxial tensile stress  $\sigma$  acting perpendicular to the crack-line (see Fig 1a) we have<sup>7</sup>

$$p_0 = \sigma \quad (13)$$

and

$$f(r) = g(-r) = 1 + \frac{1}{2r^2} + \frac{3}{2r^4} . \quad (14)$$

#### 4.2 Biaxial tensile stress

For a uniform biaxial tensile stress of  $\sigma$  and  $\alpha\sigma$  acting respectively perpendicular to and parallel to the crack-line (see Fig 1b) we have<sup>7</sup>

$$p_0 = \sigma \quad (15)$$

and

$$f(r) = g(-r) = f_1(r) + \alpha f_2(r) . \quad (16)$$

The function  $f_1(r)$  is given<sup>7</sup> by equation (14) and

$$f_2(r) = \frac{1}{2r^2} - \frac{3}{2r^4} . \quad (17)$$

#### 4.3 Point forces

For two opposing forces  $P$  (force/unit thickness) acting, diametrically opposite, at the perimeter of the hole in directions perpendicular to the crack-line (see Fig 1c) we have<sup>8</sup>

$$p_0 = \frac{P}{2R} \quad (18)$$

and

$$f(r) = g(-r) = \frac{2}{\pi} \left[ \frac{1}{r^2} + \frac{4}{(1+r^2)^2} \right] . \quad (19)$$

#### 4.4 Constant pressure

For a constant pressure  $p$  acting on the perimeter of the hole (see Fig 1d) we have<sup>8</sup>

$$p_0 = p \quad (20)$$

and

$$f(r) = g(-r) = \frac{1}{r^2} \quad (21)$$

## 5 RESULTS

Equations (11) have been solved for the four loading systems listed in section 1 and the stress intensity factors calculated from equations (12).

### 5.1 Uniaxial tensile stress

Opening-mode stress intensity factors have been obtained for the crack of length  $\ell_2$  (see Fig 1a) as a function of  $\ell_2/R$  for various values of  $\ell_1/R$ . The results are tabulated in Table 1 and shown plotted as  $K_I/(\sigma\sqrt{\pi\ell_2})$  vs  $\ell_2/R$ , for various values of  $\ell_1/R$ , in Fig 2. Table 1 also contains results for the special case when the two cracks are equal ( $\ell_1 = \ell_2$ ). The limiting value of the stress intensity factor as  $\ell_2 \rightarrow 0$  is given by

$$\lim_{\ell_2 \rightarrow 0} \left\{ \frac{K_I}{\sigma\sqrt{\pi\ell_2}} \right\} = 1.1215K_t \quad (22)$$

where  $K_t$  is the stress concentration factor at the edge of a hole diametrically opposite a radial slit. The values of  $K_t$  used in Table 1 were taken from the work of Wigglesworth<sup>9</sup>.

### 5.2 Biaxial tensile stress

The opening-mode stress intensity factor for the crack of length  $\ell_2$  (see Fig 1b) has been obtained for the remote biaxial stress field of  $\sigma$  perpendicular to the crack-line and  $\alpha\sigma$  parallel to the crack-line. The results are tabulated in Table 2 and plotted as  $K_I/(\sigma\sqrt{\pi\ell_2})$  vs  $\ell_2/R$ , for various values of  $\ell_1/R$ , in Fig 3. The special case of equal-length cracks ( $\ell_1 = \ell_2$ ) is also included in Table 2. Stress intensity factors  $K(\alpha)$  for an arbitrary biaxial stress field, *ie*  $\sigma$  perpendicular to the crack and  $\alpha\sigma$  parallel to the crack, may be obtained by a linear combination of the results for  $\alpha = 1$  with the uniaxial results ( $\alpha = 0$ ) as follows:

$$K(\alpha) = (1 - \alpha)K(0) + \alpha K(1) \quad (23)$$

### 5.3 Point forces

The values of the opening-mode stress intensity factor for a crack of length  $\ell_2$  at the edge of a hole subjected to opposing point forces  $P$  (see Fig 1c) are tabulated in Table 3 for various values of  $\ell_1$ ; results for the special case of equal-length cracks ( $\ell_1 = \ell_2$ ) are also included. Curves of  $K_I/(p_0 \sqrt{\pi \ell_2})$  vs  $\ell_2/R$  are shown in Fig 4 for various values of  $\ell_1/R$ ; in this case  $p_0 = P/(2R)$ , the 'bearing pressure'.

### 5.4 Constant pressure

For a case of a constant pressure  $p_0$  in the hole, but not in the cracks, the stress intensity factor has been evaluated for the crack of length  $\ell_2$ . Values are tabulated in Table 4 and plotted as  $K/(p_0 \sqrt{\pi \ell_2})$  vs  $\ell_2/R$ , in Fig 5, for various values of  $\ell_1/R$ . Results for the special case of  $\ell_1 = \ell_2$  are also included in Table 4.

## 6 DISCUSSION

The accuracy of the numerical procedure adopted in section 3 to solve the integral equations is good; the results are accurate to <0.1% for  $m = 20$ . An advantage of the method used in this Report is that accurate results are obtained for the important region of short cracks without the need for any special procedures as are required in some other numerical methods.

Stress intensity factors for values of  $\ell_1/R$  not contained in this Report for both uniaxial and biaxial stresses can best be obtained by interpolation of the function  $K/(\sigma \sqrt{\pi a})$ , where  $2a$  is the total crack-length from tip-to-tip, *ie*

$$2a = \ell_1 + 2R + \ell_2 . \quad (24)$$

Values of  $K_I/(\sigma \sqrt{\pi a})$  are tabulated as a function of  $\ell_2/R$  for the various values of  $\ell_1/R$  for both uniaxial and biaxial applied stress in Tables 5 and 6 respectively. It can be seen from the tables that for a given value of  $\ell_2/R$  the value of  $K_I/(\sigma \sqrt{\pi a})$  is not very dependent on  $\ell_1/R$ . This means that the total length of the crack  $2a$  (which includes the hole diameter) is an important parameter in determining the stress intensity factor. The stress intensity factor can be written as

$$K_I = Y_2 \sigma \sqrt{\pi (\ell_1 + 2R + \ell_2)/2} \quad (25)$$

for two cracks and as

$$K_I = Y_1 \sigma \sqrt{\pi(2R + \ell_2)/2} \quad (26)$$

for one crack. Thus from equations (25) and (26),

$$\frac{K_I(\text{two})}{K_I(\text{one})} = \frac{Y_2}{Y_1} \sqrt{\frac{2R + \ell_2}{\ell_1 + 2R + \ell_2}} \quad (27)$$

The approximate relationship,

$$K_I(\text{two}) \simeq \sqrt{\frac{2R + \ell_2}{\ell_1 + 2R + \ell_2}} K_I(\text{one}) \quad (28)$$

has been suggested by several authors for the case  $\ell_1 = \ell_2$  (see for example Broek<sup>5</sup>); this relationship assumes that  $Y_2/Y_1$  is unity. From the values of  $Y_2$  and  $Y_1$ , given in Tables 5 and 6, the ratio  $Y_2/Y_1$  has been calculated and is plotted in Fig 6 for both uniaxial and biaxial applied stresses. The curves of  $Y_2/Y_1$  vs  $\ell_2/R$  are plotted for various values of  $\ell_1/R$ . It can be seen that  $Y_2/Y_1$  is close to unity for the data considered and therefore equation (28) can be applied to the crack of length  $\ell_2$  for  $\ell_1 \neq \ell_2$ . For the uniaxial stress case the deviation from unity is less than 5% for  $\ell_2/R < 0.5$  and less than 10% for  $\ell_2/R < 2.0$ . For biaxial stressing the ratio  $Y_2/Y_1$  has a minimum at  $\ell_2/R \simeq 0.5$ ; for all the data considered the deviation from unity is between +3% and -4%.

The Y-functions defined in equations (25) and (26) relate the stress intensity factors for a crack at an unloaded hole to that for an isolated crack (ie  $\sigma\sqrt{\pi a}$ ). In a similar manner Y-functions can be defined for a crack at a loaded hole. Thus

$$K_I = Y_2 \frac{P}{\sqrt{\pi a}} \sqrt{\frac{\ell_1 + R}{\ell_2 + R}} \quad (2a = \ell_1 + 2R + \ell_2) \quad (29)$$

where  $P$  is the force per unit thickness. The stress intensity factor for one of the tips of an isolated crack of length  $2a$  subjected to forces  $P$  acting on opposite faces of the crack, a distance  $\ell_2 + R$  from the considered tip and  $\ell_1 + R$  from the other tip, is given by

$$K_I = \frac{P}{\sqrt{\pi a}} \sqrt{\frac{\ell_1 + R}{\ell_2 + R}} \quad (30)$$

The values of the Y-functions are tabulated, as a function of  $\ell_2/R$  for various values of  $\ell_1/R$ , in Tables 7 and 8 for the point force  $P$  and the internal pressure  $p_0$  respectively. In the case of the internal pressure the force is equal to  $2p_0R$ . As in the case of remote stressing conditions the Y-functions are not very dependent on  $\ell_1/R$ ; thus these data can be used to interpolate values of the stress intensity factor for any value of  $\ell_1/R$  not contained in the results reported.

From equation (29) it follows that, for two cracks,

$$K_I = Y_2 \frac{P}{\sqrt{\pi}} \sqrt{\frac{2(\ell_1 + R)}{(\ell_1 + 2R + \ell_2)(\ell_2 + R)}} \quad (31)$$

and for one crack

$$K_I = Y_1 \frac{P}{\sqrt{\pi}} \sqrt{\frac{2R}{(2R + \ell_2)(\ell_2 + R)}} \quad (32)$$

Thus

$$\frac{K_I(\text{two})}{K_I(\text{one})} = \frac{Y_2}{Y_1} \sqrt{\frac{(\ell_1 + R)(2R + \ell_2)}{R(\ell_1 + 2R + \ell_2)}} \quad (33)$$

Equation (33) is similar in form to equation (27) which suggests a similar approximation to that in equation (28) for estimating the stress intensity factors for the crack of length  $\ell_2$  when  $\ell_1 \neq 0$  from that for a crack of length  $\ell_2$  when  $\ell_1 = 0$ . The approximation is

$$\frac{K_I(\text{two})}{K_I(\text{one})} \approx \sqrt{\frac{(\ell_1 + R)(2R + \ell_2)}{R(\ell_1 + 2R + \ell_2)}} \quad (34)$$

This approximation assumes that  $Y_2/Y_1 \approx 1$ ; the errors involved in this assumption can be seen from Fig 6 where  $Y_2/Y_1$  vs  $\ell_2/R$  is plotted for various

values of  $l_1/R$  for both point loads and uniform pressure on the hole. For point loads the maximum deviation of  $Y_2/Y_1$  from unity occurs for  $l_1/R = 0.5$ ; the deviation varies from -4% for small  $l_2/R$  values to -7% for large values of  $l_2/R$ . For uniform pressure the deviations are between  $\pm 6\%$  for  $l_2/R < 1.0$  and  $l_1/R < 10$ ; for large values of  $l_2/R$  deviations are greater, -13% for  $l_1/R = l_2/R = 10$ .

The simple approximate relationships for obtaining opening-mode stress intensity factors for two cracks from those of one crack for both remote and local loading would still apply if the loading was not symmetrical about the crack-line. Crack problems with asymmetrical loading about the crack-line are more difficult to solve, particularly if there are two cracks of unequal length. However, some solutions for a single crack under remote loading<sup>10,11</sup> and localized loading<sup>11,12</sup> are available and could be used to obtain approximate opening-mode stress intensity factors for two-crack problems.

#### 7 CONCLUSIONS

- (1) Accurate opening-mode stress intensity factors have been obtained for cracks at the edges of a circular hole in sheets subjected to either remote tensile stresses or loads on the perimeter of the hole.
- (2) An approximate technique for obtaining stress intensity factors for two cracks from values for a single crack has been investigated and the errors in the approximation shown to be small (a few per cent).
- (3) The approximate technique could be extended to other configurations for which only single crack results are known.

Table 1  
 $K_I / (\sigma\sqrt{\pi\ell_2})$  FOR CRACK OF LENGTH  $\ell_2$  IN UNIAXIAL  
 STRESS FIELD ( $\alpha = 0$ )

$\ell_1/R$ \ / $\ell_2/R$	0.0	0.5	1.0	2.0	5.0	10.0	$\ell_1 = \ell_2$
0.00	3.364	-	-	4.29	5.41	6.82	3.364
0.01	3.291	3.490	3.749	4.216	5.324	6.708	3.293
0.02	3.223	3.418	3.672	4.130	5.216	6.574	3.225
0.05	3.036	3.220	3.460	3.893	4.920	6.206	3.041
0.10	2.771	2.941	3.161	3.558	4.501	5.685	2.786
0.15	2.555	2.711	2.915	3.282	4.156	5.254	2.581
0.20	2.373	2.520	2.710	3.052	3.866	4.892	2.412
0.30	2.092	2.221	2.388	2.690	3.410	4.320	2.156
0.50	1.727	1.832	1.968	2.213	2.803	3.555	1.832
0.70	1.517	1.595	1.710	1.918	2.423	3.070	1.642
1.00	1.306	1.378	1.471	1.643	2.061	2.604	1.472
1.5	1.127	1.182	1.254	1.388	1.719	2.156	1.323
2.0	1.030	1.075	1.134	1.244	1.522	1.893	1.244
3.0	0.930	0.962	1.005	1.087	1.300	1.590	1.163
5.0	0.845	0.866	0.895	0.950	1.098	1.306	1.098
10.0	0.779	0.790	0.806	0.836	0.922	1.049	1.049

Table 2  
 $K_I(\sigma\sqrt{\pi\ell_2})$  FOR CRACK OF LENGTH  $\ell_2$  IN BIAXIAL  
STRESS FIELD ( $\alpha = 1$ )

$\ell_1/R$ $\ell_2/R$	0.0	0.5	1.0	2.0	5.0	10.0	$\ell_1 = \ell_2$
0.01	2.212	2.369	2.604	3.057	4.168	5.562	2.212
0.02	2.183	2.337	2.567	3.012	4.101	5.468	2.184
0.05	2.104	2.249	2.466	2.886	3.917	5.211	2.106
0.10	1.988	2.122	2.321	2.706	3.652	4.843	1.998
0.15	1.891	2.015	2.199	2.554	3.430	4.534	1.909
0.20	1.807	1.923	2.094	2.425	3.240	4.272	1.835
0.30	1.671	1.773	1.924	2.215	2.935	3.850	1.719
0.50	1.480	1.564	1.685	1.922	2.511	3.266	1.564
0.70	1.358	1.423	1.526	1.727	2.229	2.879	1.464
1.00	1.226	1.283	1.367	1.532	1.948	2.492	1.367
1.5	1.097	1.142	1.207	1.335	1.664	2.102	1.272
2.0	1.020	1.056	1.110	1.216	1.491	1.862	1.216
3.0	0.932	0.958	0.998	1.077	1.288	1.579	1.152
5.0	0.850	0.868	0.894	0.948	1.095	1.303	1.095
10.0		0.792	0.807	0.837	0.922	1.049	1.049

Table 3  
 $K_I / (p_0 \sqrt{\pi \ell_2})$  FOR CRACK OF LENGTH  $\ell_2$  WITH POINT FORCES  $P$   
 ACTING ON THE HOLE PERIMETER ( $p_0 = P/(2R)$ )

$a_1/R$ $a_2/R$	0.0	0.5	1.0	2.0	5.0	10.0	$\ell_1 = \ell_2$
0.01	1.399	1.482	1.573	1.691	1.831	1.902	1.400
0.02	1.373	1.454	1.543	1.658	1.796	1.866	1.373
0.05	1.298	1.375	1.459	1.568	1.698	1.765	1.300
0.10	1.188	1.259	1.336	1.436	1.556	1.618	1.194
0.15	1.094	1.159	1.231	1.323	1.435	1.492	1.105
0.20	1.011	1.072	1.139	1.225	1.330	1.384	1.028
0.30	0.874	0.928	0.987	1.064	1.158	1.207	0.901
0.50	0.676	0.720	0.768	0.832	0.911	0.953	0.720
0.70	0.542	0.579	0.620	0.674	0.744	0.782	0.597
1.00	0.408	0.438	0.471	0.516	0.576	0.609	0.471
1.5	0.278	0.300	0.326	0.361	0.410	0.439	0.346
2.0	0.205	0.222	0.243	0.271	0.313	0.338	0.272
4.0	0.089	0.098	0.109	0.126	0.152	0.170	0.145
6.0	0.053	0.058	0.066	0.076	0.095	0.109	0.099
10.0	0.026	0.029	0.033	0.040	0.051	0.061	0.061

Table 4  
 $K_I / (P_0 \sqrt{\pi \ell_2})$  FOR CRACK OF LENGTH  $\ell_2$  WITH A UNIFORM  
 PRESSURE  $P_0$  IN THE HOLE

$a_1/R$ $a_2/R$	0.0	0.5	1.0	2.0	5.0	10.0	$\ell_1 = \ell_2$
0.01	1.099	1.165	1.241	1.347	1.485	1.560	1.099
0.02	1.078	1.143	1.218	1.321	1.457	1.530	1.079
0.05	1.020	1.081	1.152	1.250	1.378	1.448	1.022
0.10	0.935	0.991	1.056	1.146	1.264	1.329	0.940
0.15	0.863	0.915	0.975	1.058	1.168	1.228	0.872
0.20	0.800	0.849	0.905	0.982	1.085	1.142	0.813
0.30	0.697	0.740	0.790	0.858	0.950	1.002	0.719
0.50	0.551	0.586	0.626	0.682	0.759	0.803	0.586
0.70	0.452	0.481	0.515	0.564	0.630	0.669	0.495
1.00	0.352	0.375	0.403	0.443	0.500	0.534	0.403
1.5	0.251	0.269	0.290	0.321	0.368	0.396	0.308
2.0	0.192	0.206	0.223	0.248	0.288	0.313	0.248
4.0	0.090	0.098	0.107	0.121	0.146	0.164	0.140
6.0	0.055	0.060	0.066	0.076	0.093	0.108	0.097
10.0	0.028	0.031	0.034	0.040	0.050	0.060	0.060

Table 5

 $K_I / (\sigma\sqrt{\pi a})$  FOR CRACK OF LENGTH  $\ell_2$  IN UNIAXIAL STRESS FIELD ( $\alpha = 0$ )

$$2a = \ell_1 + 2R + \ell_2$$

$\ell_1/R$ $\ell_2/R$	0.0	0.5	1.0	2.0	5.0	10.0	$\ell_1 = \ell_2$
0.00	0.000	0.000	0.000	0.000	0.000	0.000	0.000
0.01	0.328	0.312	0.306	0.298	0.284	0.274	0.328
0.02	0.454	0.431	0.422	0.412	0.394	0.379	0.452
0.05	0.667	0.638	0.626	0.618	0.586	0.565	0.663
0.10	0.853	0.816	0.803	0.786	0.756	0.731	0.840
0.15	0.953	0.912	0.900	0.882	0.851	0.826	0.932
0.20	1.013	0.970	0.958	0.942	0.911	0.886	0.985
0.30	1.067	1.028	1.018	1.005	0.977	0.954	1.035
0.50	1.091	1.058	1.052	1.043	1.024	1.006	1.058
0.70	1.082	1.055	1.052	1.047	1.033	1.019	1.053
1.00	1.066	1.041	1.040	1.039	1.031	1.022	1.041
1.5	1.044	1.024	1.024	1.025	1.021	1.016	1.025
2.0	1.030	1.013	1.014	1.016	1.014	1.012	1.016
3.0	1.018	1.004	1.005	1.007	1.007	1.006	1.007
5.0	1.010	1.000	1.000	1.001	1.002	1.002	1.002
10.0	1.005	1.000	0.999	1.000	1.000	1.000	1.000

Table 6

 $K_I / (\sigma\sqrt{\pi a})$  FOR CRACK OF LENGTH  $\ell_2$  IN BIAXIAL STRESS FIELD ( $\alpha = 1$ )

$$2a = \ell_1 + 2R + \ell_2$$

$\ell_1/R$ $\ell_2/R$	0.0	0.5	1.0	2.0	5.0	10.0	$\ell_1 = \ell_2$
0.00	0.000	0.000	0.000	0.000	0.000	0.000	0.000
0.01	0.220	0.211	0.212	0.216	0.223	0.227	0.220
0.02	0.308	0.294	0.295	0.300	0.310	0.315	0.306
0.05	0.462	0.445	0.447	0.454	0.466	0.474	0.460
0.10	0.612	0.589	0.590	0.598	0.613	0.623	0.602
0.15	0.706	0.678	0.678	0.687	0.703	0.712	0.690
0.20	0.772	0.740	0.740	0.748	0.764	0.774	0.749
0.30	0.852	0.821	0.820	0.827	0.841	0.850	0.826
0.50	0.935	0.903	0.901	0.906	0.917	0.924	0.903
0.70	0.970	0.941	0.939	0.942	0.951	0.956	0.940
1.00	1.000	0.970	0.967	0.969	0.974	0.978	0.967
1.5	1.016	0.989	0.985	0.986	0.989	0.991	0.985
2.0	1.020	0.996	0.993	0.993	0.994	0.995	0.993
3.0	1.020	1.001	0.998	0.997	0.997	0.998	0.997
5.0	1.016	1.003	1.000	0.999	0.999	1.000	0.999
10.0	1.009	1.002	1.000	1.000	1.000	1.000	1.000

Table 7

$$K_I \sqrt{\frac{P}{\sqrt{\pi a}} \sqrt{\frac{\ell_1 + R}{\ell_2 + R}}} \quad \text{FOR CRACK OF LENGTH } \ell_2 \quad \text{WITH POINT FORCES } P \quad \text{ACTING}$$

ON HOLE PERIMETER:

$$2a = \ell_1 + 2R + \ell_2$$

$a_1/R$	$a_2/R$	0.001	0.5	1.0	2.0	5.0	10.0
0.01	0.221	0.221	0.213	0.215	0.218	0.221	0.222
0.02	0.309	0.309	0.299	0.300	0.304	0.308	0.309
0.05	0.473	0.473	0.456	0.459	0.464	0.468	0.470
0.10	0.634	0.634	0.610	0.613	0.618	0.624	0.625
0.15	0.739	0.739	0.710	0.712	0.718	0.723	0.724
0.20	0.816	0.816	0.782	0.783	0.789	0.793	0.793
0.30	0.914	0.914	0.879	0.879	0.883	0.886	0.885
0.50	1.029	1.029	0.979	0.978	0.980	0.979	0.977
0.70	1.080	1.080	1.025	1.022	1.023	1.021	1.018
1.00	1.111	1.111	1.051	1.047	1.047	1.044	1.040
1.5	1.120	1.120	1.056	1.052	1.052	1.049	1.045
2.0	1.114	1.114	1.048	1.044	1.045	1.043	1.039
4.0	1.088	1.088	1.017	1.015	1.019	1.020	1.018
6.0	1.074	1.074	1.002	1.001	1.006	1.010	1.008
10.0	1.063	1.063	0.989	0.988	0.995	1.001	1.000

Table 8

$$K_I / \left[ \frac{2p_0 R}{\sqrt{\pi a}} \sqrt{\frac{\ell_1 + R}{\ell_2 + R}} \right] \text{ FOR CRACK OF LENGTH } \ell_2 \text{ WITH A UNIFORM PRESSURE}$$

$p_0$  IN THE HOLE:

$$2a = \ell_1 + 2R + \ell_2$$

$a_1/R$ $a_2/R$	0.001	0.5	1.0	2.0	5.0	10.0
0.01	0.174	0.168	0.170	0.174	0.179	0.182
0.02	0.243	0.235	0.237	0.243	0.250	0.254
0.05	0.372	0.359	0.362	0.370	0.380	0.386
0.10	0.499	0.481	0.484	0.494	0.506	0.513
0.15	0.583	0.561	0.564	0.574	0.588	0.595
0.20	0.646	0.620	0.623	0.632	0.647	0.654
0.30	0.733	0.701	0.704	0.713	0.727	0.735
0.50	0.838	0.797	0.796	0.804	0.816	0.823
0.70	0.899	0.851	0.842	0.854	0.865	0.871
1.0	0.956	0.900	0.895	0.898	0.906	0.911
1.5	1.010	0.945	0.926	0.936	0.942	0.945
2.0	1.042	0.969	0.958	0.956	0.959	0.961
4.0	1.098	1.010	0.993	0.985	0.984	0.984
6.0	1.121	1.024	1.004	0.994	0.991	0.990
10.0	1.140	1.035	1.013	1.001	0.995	0.994

LIST OF SYMBOLS

$a$	crack-length ( $2a =$ tip-to-tip distance)
$b, c$	crack tips located at $r = b, c$
$f(r), f_1(r), f_2(r)$	loading functions (dimensionless)
$g(r)$	loading function (dimensionless)
$h(t)$	function defined by equation (3)
$h(-b), h(c)$	end-point values of $h(t)$
$j, k$	suffices; $j = 1, 2, \dots, m, k = 1, 2, \dots, m - 1$
$K_I$	opening-mode stress intensity factor
$K_b, K_c$	values of $K_I$ at tips $b$ and $c$ respectively
$K_t$	stress <i>concentration</i> factor
$k(r, t)$	non-singular function defined by equation (6)
$l_1$	crack-length = $R(b - 1)$
$l_2$	crack-length = $R(c - 1)$
$m$	number of integration points (section 3)
$M(r, t)$	singular kernel in equation (3)
$P$	force per unit thickness
$P_0$	stress constant
$r$	dimensionless radial coordinate ( $= \rho/R$ )
$r_j$	discrete values of $r$
$R$	radius of hole
$t$	variable of integration in equation (3)
$t_j$	discrete values of $t$
$u_j$	defined by equation (7)
$v_j$	defined by equation (8)
$Y_1, Y_2$	geometric factors for one and two cracks respectively
$\alpha$	ratio of biaxial stresses
$\rho$	polar coordinates
$\theta$	
$\sigma_{\theta\theta}$	stress component
$\sigma$	applied stress

## REFERENCES

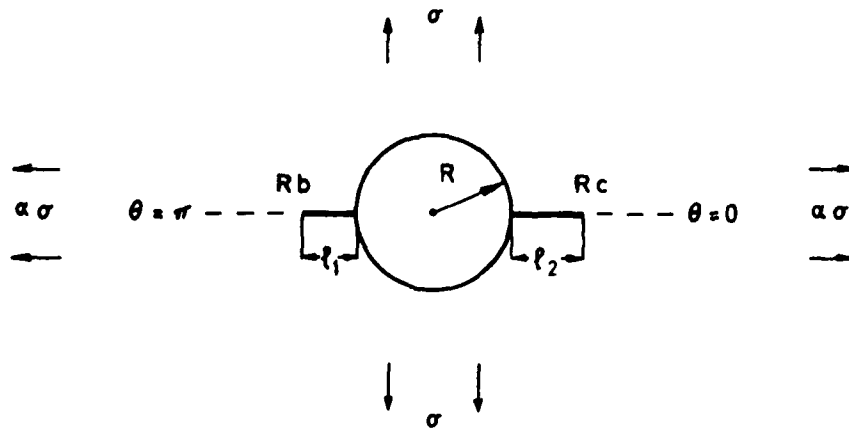
- | <u>No.</u> | <u>Author</u>            | <u>Title, etc</u>   |
|------------|--------------------------|---|
| 1          | W.T. Kirkby              | Examples of aircraft failure in <i>Fracture mechanics of aircraft structures</i> .<br>Edited by H. Liebowitz, AGARDograph No 176,<br>AGARD (1974)                                       |
| 2          | O.L. Bowie               | Analysis of an infinite plate containing radial cracks originating at the boundary of an internal circular hole.<br><i>J. Math. Phys.</i> , <u>35</u> , 60-71 (1956)                    |
| 3          | J. Tweed<br>D.P. Rooke   | The distribution of stress near the tip of a radial crack at the edge of a circular hole.<br><i>Int. J. Engng. Sci.</i> , <u>11</u> , 1185-1195 (1973)                                  |
| 4          | J. Tweed<br>D.P. Rooke   | The elastic problem for an infinite solid containing a circular hole with a pair of radial edge cracks of different lengths.<br><i>Int. J. Engng. Sci.</i> , <u>14</u> , 925-933 (1976) |
| 5          | D. Broek                 | <i>Elementary engineering fracture mechanics</i> .<br>Chap 14, Leyden, Noordhoff (1974)   |
| 6          | F. Erdogan<br>G.D. Gupta | On the numerical solution of singular integral equations.<br><i>Quart. Appl. Maths.</i> , <u>29</u> , 525-534 (1972)  |
| 7          | I.S. Sokolnikoff         | <i>Mathematical theory of elasticity</i> .<br>2nd Ed, New York, McGraw-Hill (1956)  |
| 8          | A.E. Green<br>W. Zerna   | <i>Theoretical elasticity</i> .<br>Oxford, Clarendon Press (1968)   |
| 9          | L.A. Wigglesworth        | Stress relief in a cracked plate.<br><i>Mathematika</i> , <u>5</u> , 67-81 (1958)   |
| 10         | Y.C. Hsu                 | The infinite sheet with cracked cylindrical hole under inclined tension or in-plane shear.<br><i>Int. J. Fract.</i> , <u>11</u> , 571-581 (1975)  |
| 11         | J. Tweed<br>D.P. Rooke   | The stress intensity factor for a crack at the edge of a loaded hole.<br><i>Int. J. Engng. Sci.</i> , (to be published 1979)  |

REFERENCES (concluded)

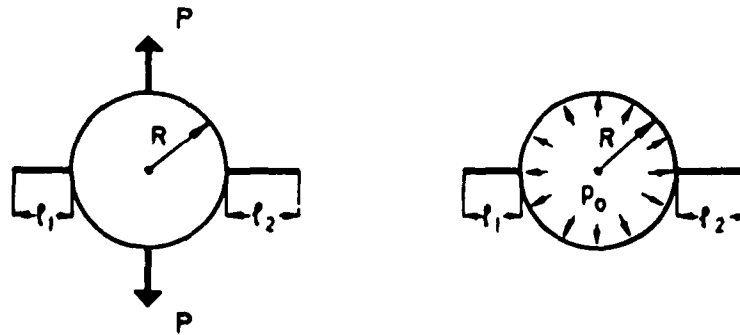
- | <u>No.</u> | <u>Author</u>          | <u>Title, etc</u>  |
|------------|------------------------|--|
| 12         | D.P. Rooke<br>J. Tweed | Stress intensity factors for a crack at the edge of a pressurized hole.<br>To be presented at 16th Annual Meeting of Society of Engineering Science Inc., Northwestern University, Evanston, Ill. (5-7 September 1979) |

B. ... ..

Fig 1



Uniaxial ( $\alpha=0$ ) or biaxial ( $\alpha \neq 0$ ) tensile stress remote from the hole



Point forces on hole perimeter

Uniform pressure in hole

Fig 1 Load distributions

Fig 2

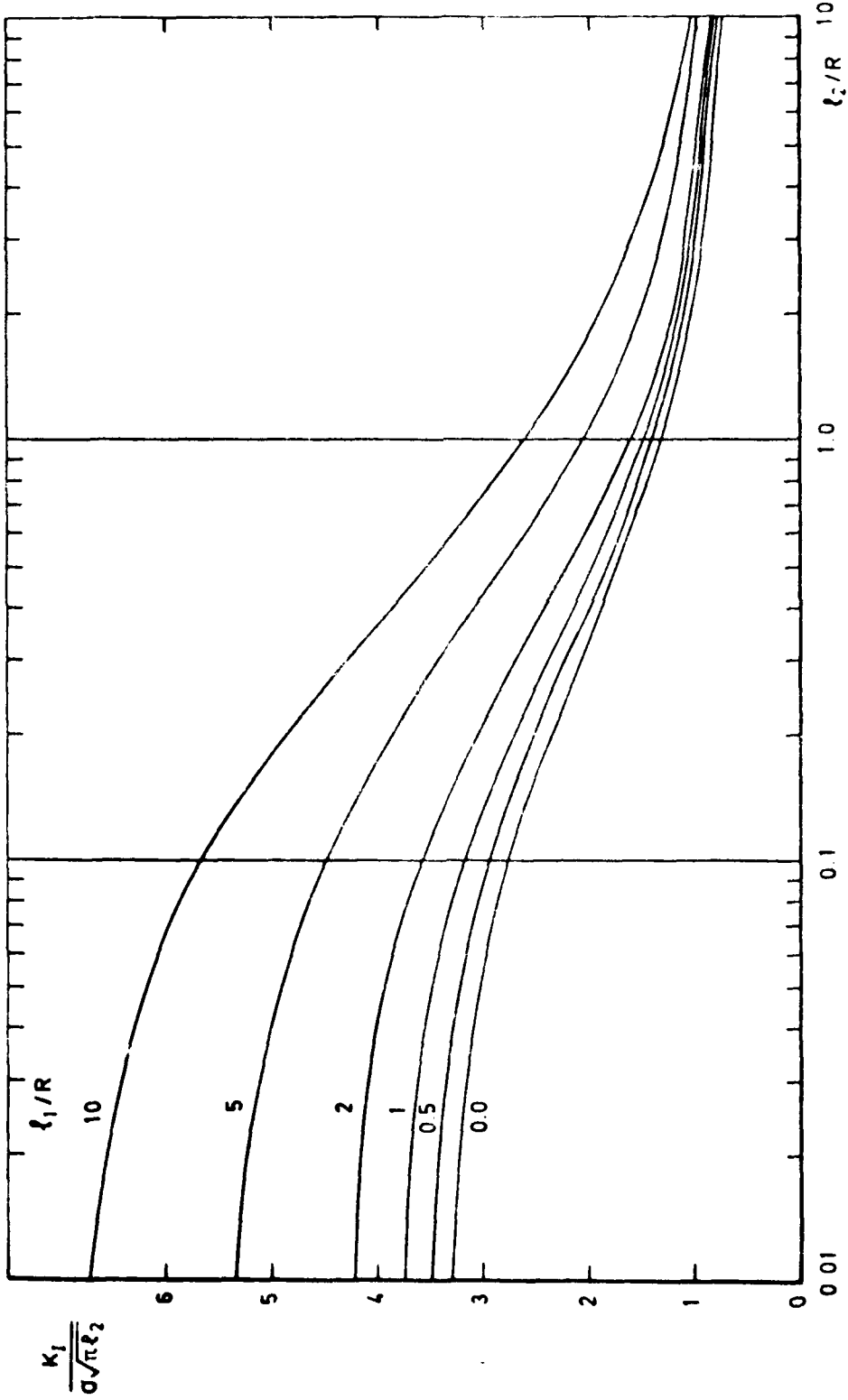


Fig 2 The stress intensity factor for a uniaxial ( $\alpha = 0$ ) applied stress

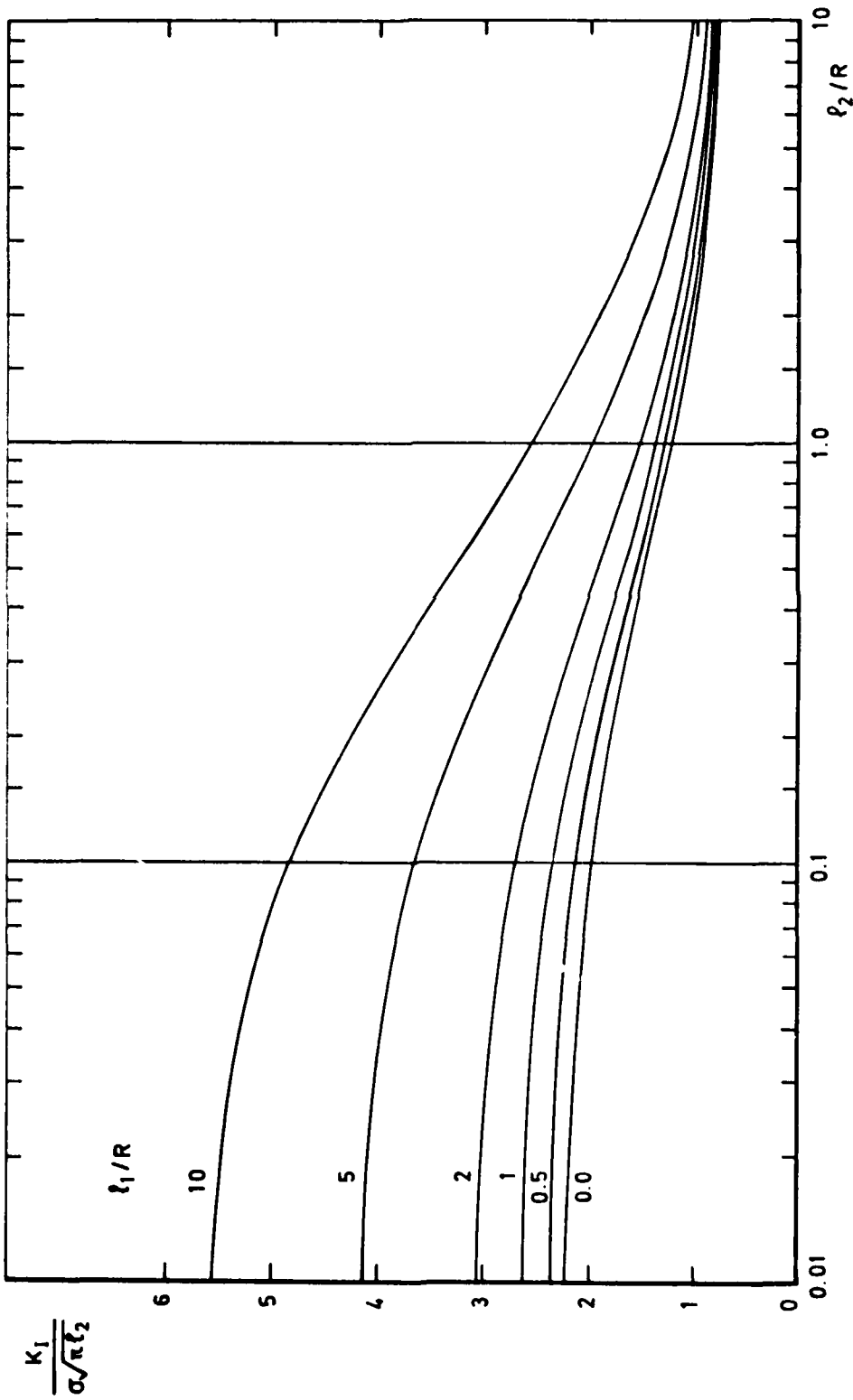


Fig 3 The stress intensity factor for a biaxial ( $\alpha = 1$ ) applied stress

Fig 3

Fig 4

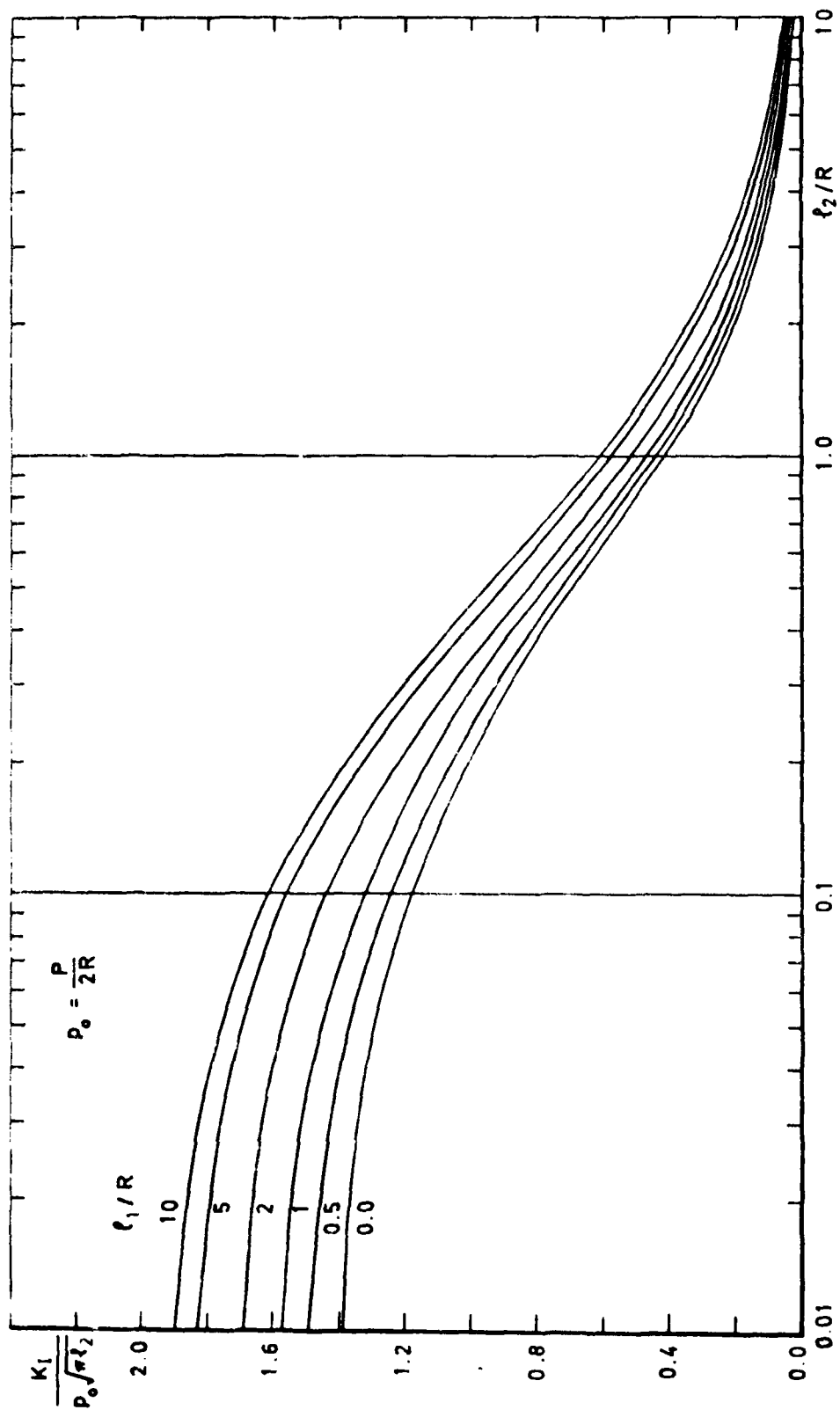


Fig 4 The stress intensity factor for point forces

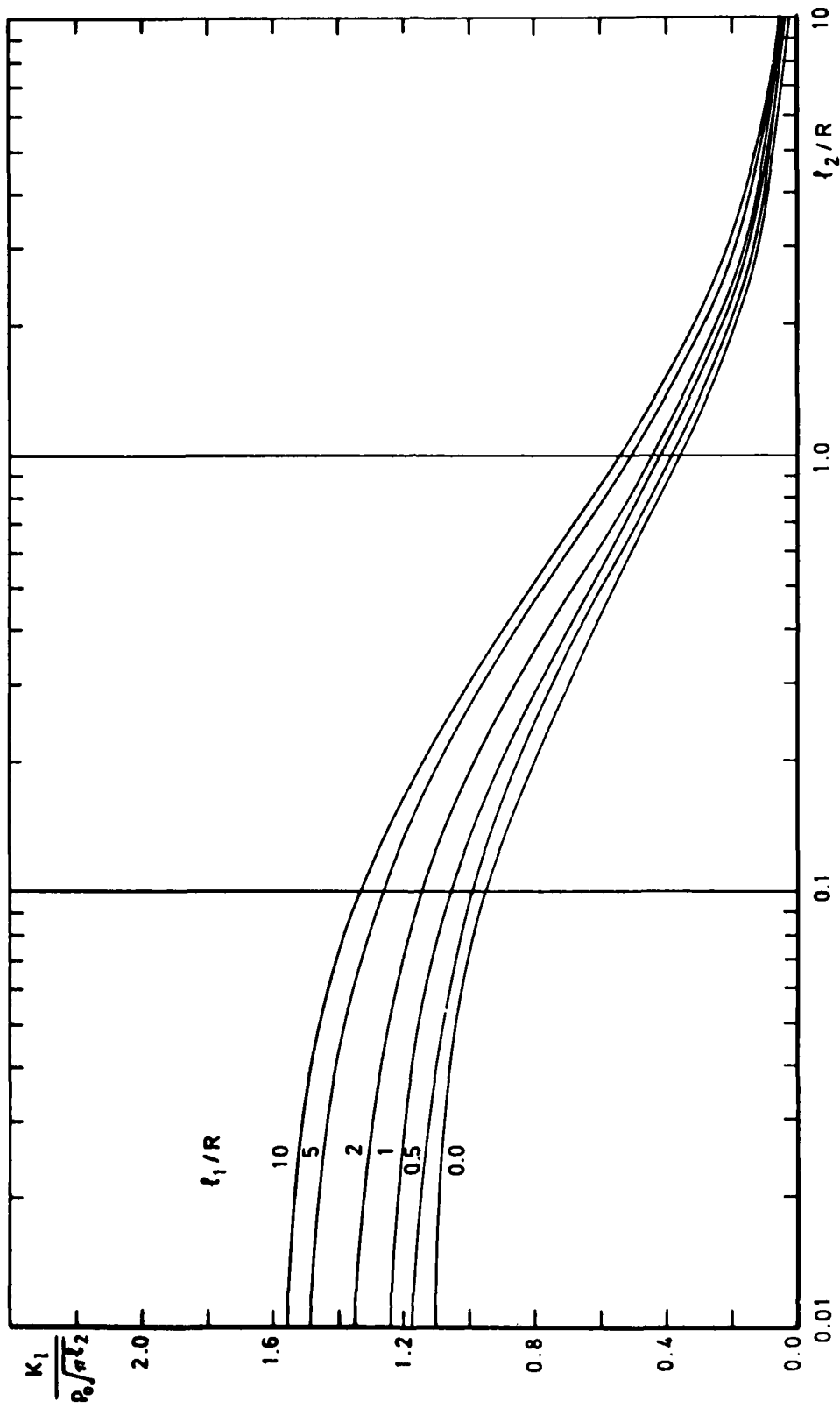


Fig 5 The stress intensity factor for uniform pressure

Fig 6

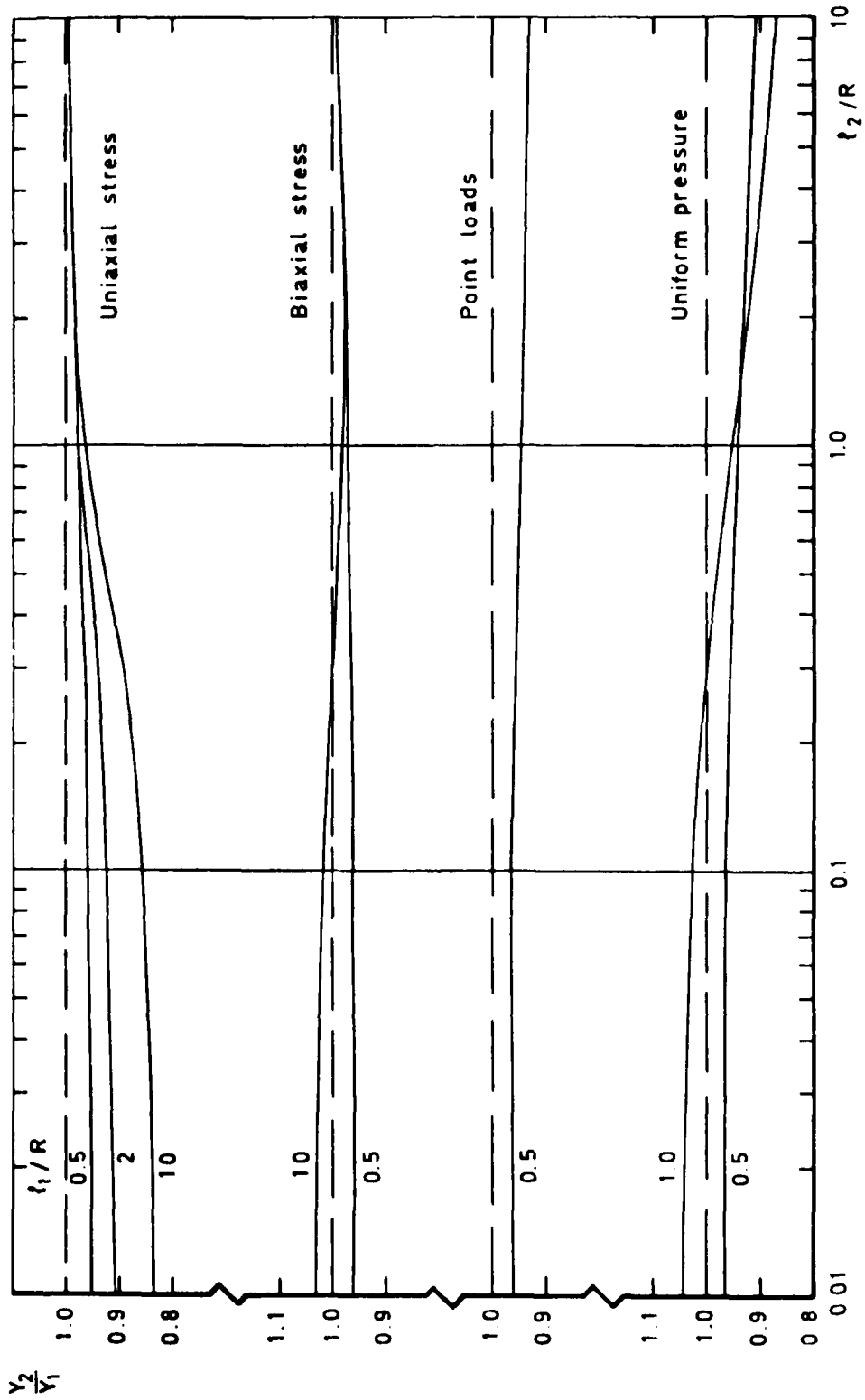


Fig 6 Ratio of geometric factors for two cracks and one crack at the edge of a hole

